

Entering the overcritical regime of nonlinear Breit-Wheeler pair production in collisions of bremsstrahlung γ -rays and superintense, tightly focused laser pulses

I. Elsner,^{*} A. Golub,[†] S. Villalba-Chávez,[‡] and C. Müller[§]
*Institut für Theoretische Physik I, Heinrich-Heine-Universität Düsseldorf,
Universitätsstraße 1, 40225 Düsseldorf, Germany.*

(Dated: January 16, 2025)

Near-future high-intensity lasers offer prospects for the observation of nonlinear Breit-Wheeler pair production in an overcritical field regime, where the quantum nonlinearity parameter substantially exceeds unity. This experimentally yet unexplored scenario is envisaged here to be reached via the collision of a tightly focused laser pulse with high-energy bremsstrahlung photons. We calculate the achievable number of positrons in a range of laser intensities around 10^{23} W/cm² and GeV-energies of the incident bremsstrahlung-generating electron beam. We investigate under which conditions the attenuation of the γ -beam due to the production process must be taken into account. In the considered interaction regime, where the local production rate grows rather moderately with higher field intensities, it is shown that the range of mostly contributing bremsstrahlung frequencies is generally very broad. For sufficiently large values of the quantum nonlinearity parameter, an optimum domain of frequencies emerges which is located far below the spectral endpoint. Furthermore, we show that it is beneficial for achieving the optimum pair yield to increase the interaction volume by a wider laser focus at the expense of decreased field intensity.

I. INTRODUCTION

Creation of electron-positron pairs from vacuum in the presence of very strong electromagnetic fields belongs to the most dramatic predictions of quantum electrodynamics. After a few seminal studies in the early days of relativistic quantum mechanics [1], the availability of laser radiation starting in the 1960s has sparked sustained interest of theoreticians in the subject [2–8].

In particular, a nonlinear version of the Breit-Wheeler effect was studied (see [8–10] and references therein) where pairs are produced by multiphoton absorption in the collision of a high-energy gamma photon with an intense laser wave, according to the reaction $\omega' + n\omega \rightarrow e^+e^-$, where n denotes the number of absorbed low-frequency laser photons. Various interaction regimes of the process have been identified that are distinguished by the values of two dimensionless parameters: on the one hand, the classical intensity parameter $\xi = |e\mathcal{E}_0|/(m\omega)$, with the laser frequency ω and its peak field strength \mathcal{E}_0 ; and on the other hand, the quantum nonlinearity parameter given by $\kappa = 2\omega'\mathcal{E}_0/(mE_c)$, with the critical Schwinger field $E_c = m^2/|e| \approx 1.3 \times 10^{16}$ Vcm⁻¹ and assuming a counterpropagating beam geometry. Besides, e and m denote the electron charge and mass, respectively. The theoretical treatment in the seminal papers [2–4] relied on monoenergetic gamma photons and a plane-wave description of the laser field. In the 1990s, the nonlinear Breit-Wheeler process has been observed experimentally in a few-photon regime ($n \sim 5$) at $\xi \lesssim 1$, where the process rate was found to follow a power law of the form

$$R \sim \xi^{2n} [11].$$

Due to the ongoing progress in high-intensity laser technology, the experimental interest in the nonlinear Breit-Wheeler process is currently revived [12–15] – which is accompanied by corresponding theoretical efforts [16–30]. The aim is to probe the hitherto unobserved regimes with $\xi \gg 1$ where the rate exhibits a manifestly nonperturbative dependence on the external field strength. For $\kappa \ll 1$, it has a tunneling-like exponential form $R \sim e^{-8/(3\kappa)}$, whereas for $\kappa \gg 1$ the rate scales as $R \sim \kappa^{2/3}$ [8]. Since strong focusing is required to achieve laser pulses with such high intensities, it is crucial in calculations to properly account for the spatiotemporal structure of the fields [31–34].

A promising possibility to generate high-energy gamma rays is offered by bremsstrahlung of highly relativistic electrons from high- Z targets, as proposed by Reiss in the 1970s [5], and recently further investigated by several groups [32–39]. In this situation, the gamma photons are not monoenergetic but span a broad range of energies. This route is followed in the experimental designs for nonlinear Breit-Wheeler pair creation at CALA [13] and DESY [14]. If successful, they could be considered as ‘discovery experiments’ for the highly nonlinear regime of the strong field Breit-Wheeler process, which will be followed afterwards by ‘precision experiments’ that aim at covering large regions of the parameter space with enhanced accuracy. A detailed theoretical analysis of the experiment planned at CALA has recently been carried out [33, 34], including laser focusing effects and the broad frequency spectrum of bremsstrahlung. This experiment is going to operate in the $\xi \gg 1$ regime with $\kappa \sim 1$, exploiting laser wakefield accelerated incident electrons of about 2.5 GeV energy to generate the bremsstrahlung in a tungsten target [13].

In the present paper, we extend the previous analysis [33] to the overcritical regime of large κ values up

^{*} ingo.elsner@hhu.de

[†] alina.golub@hhu.de

[‡] selym@tp1.hhu.de

[§] c.mueller@tp1.hhu.de

to $\kappa \approx 30$. It could, for instance, be realized in the future at the Extreme Light Infrastructure (ELI) [15] or CoReLS [40] facilities. Our main goal is to reveal characteristic differences between the intermediate ($\kappa \approx 1$) and overcritical ($\kappa \gg 1$) regimes of the nonlinear strong-field Breit-Wheeler process with focused laser pulses and gamma photons from bremsstrahlung.¹ We will show that the overcritical field regime requires an adjusted theoretical approach and exhibits qualitatively distinct properties in terms of its scaling behaviours. This affects, in particular, its dependencies on the laser pulse duration and focusing as well as the mainly contributing spectral range of gamma photons. Our outcomes can be relevant for the design of future experiments.

It is worth noting that the overcritical regime of strong-field pair production can also be probed when an incident high-energy electron beam interacts directly with an ultrastrong laser pulse [12, 42, 43]. In this case, however, the electron beam can be strongly distorted by radiation reaction effects before reaching the focal region of highest field strength. In this regard, the use of a target foil that first converts the incident electron energy in a controlled way into γ photons, which afterwards penetrate into the laser focal region, offers certain advantages. Figure 1 shows a scheme of the envisaged setup.

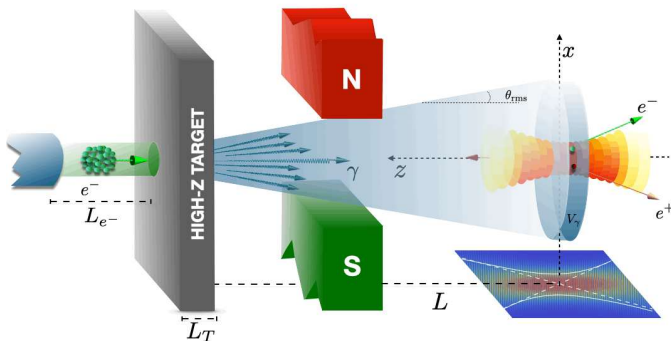


FIG. 1. Scheme of the experimental setup for entering the overcritical regime of the nonlinear Breit-Wheeler pair production process from the collision of bremsstrahlung gamma photons and a high-intensity laser pulse. The collision of a monoenergetic electron beam with a narrow high- Z target will result in the bremsstrahlung burst utilized in the setup. A magnet after the target will deflect residual electrons away from the site where the photon-photon collision occurs.

Our study is presented as follows: In Sec. II we first briefly review the theoretical description of Breit-Wheeler pair creation in collisions of bremsstrahlung γ -rays with a focussed high-intensity laser pulse from

Ref. [33] and, afterwards, extend it to the overcritical regime. Next, in Sec. III, our numerical results obtained for the overcritical regime $\kappa > 1$ are discussed and put in contrast to the properties of the pair creation process at $\kappa \approx 1$. Finally, the conclusions are drawn in the last section. Throughout the manuscript, the Lorentz-Heaviside units [$c = \hbar = \epsilon_0 = 1$], and the metric tensor with the signature $\text{diag}(g^{\mu\nu}) = (1, -1, -1, -1)$ are used.

II. THEORETICAL TREATMENT

As the discussion in this manuscript aims at pair production at high laser intensities with $\xi \gg 1$, the locally constant field approximation is applicable [8, 25]. Under such a condition, the formation length $l \sim \lambda/(\xi\pi)$ is much smaller than the laser wavelength $\lambda = 2\pi\omega^{-1}$, evidencing that the pairs are created in regions where the background is nearly a constant crossed field. Accordingly, the rate of the process per γ -photon can be approximated locally by the one linked to pair production in a crossed field configuration [3, 8]

$$R(\kappa) = -\frac{\alpha m^2}{6\sqrt{\pi}\omega'} \int_1^\infty \frac{du(8u+1)}{u\sqrt{u(u-1)}} \frac{\Phi'(z)}{z}, \quad (1)$$

where the local value $\kappa = \kappa(\vec{r}, t)$ of the quantum non-linearity parameter at the considered space-time point must be inserted. Here, $\alpha = e^2/(4\pi) \approx 1/137$ is the fine structure constant, $z = (4u/\kappa)^{2/3}$ and $\Phi'(z)$ stands for the derivative of the Airy function $\Phi(z) = \frac{1}{\sqrt{\pi}} \int_0^\infty dt \cos(\frac{t^3}{3} + zt)$.

Equation (1) forms the basis for two different theoretical approaches to strong-field Breit-Wheeler pair production that will be outlined in Secs. II B and II C below. Beforehand, we shall describe the colliding high-intensity focussed laser pulse and high-energy bremsstrahlung γ -rays.

A. Descriptions of the focussed laser pulse and bremsstrahlung spectrum

The laser field shall be taken as a tightly focused Gaussian pulse in the paraxial approximation. A geometry is chosen in which this strong background propagates in z -direction and is linearly polarized along the x -axis. The corresponding electric field reads [44]

$$E_x = \mathcal{E}_0 \frac{e^{-\left(\sqrt{2\ln(2)}\frac{(t-z)}{\tau}\right)^2}}{\sqrt{1+\zeta(z)^2}} e^{-\left(\frac{\rho}{w(z)}\right)^2} \sin(\Phi), \quad (2)$$

where τ stands for the pulse duration (at FWHM from the intensity), $\rho^2 = x^2 + y^2$, $\zeta = z/z_R$ with the Rayleigh length $z_R = \pi w_0^2/\lambda$ and the beam waist radius at the focus w_0 , whereas $w(z) = w_0\sqrt{1+\zeta(z)^2}$. Moreover,

¹ The κ values considered here remain far below the domain where perturbation theory with respect to the quantized radiation field is expected to break down, i.e. $\kappa \ll \alpha^{-3/2} \approx 1.6 \times 10^3$, with α referring to the fine-structure constant [8–10, 41].

$E_x = B_y$ holds and the field phase reads

$$\Phi = \omega(t - z) - \zeta(z) \frac{\rho^2}{w^2(z)} + \arctan(\zeta). \quad (3)$$

It is worth remarking that the spacetime dependent quantum nonlinearity parameter $\kappa = |e| \sqrt{-(F_{\mu\nu} k'^{\nu})^2} / m^3$, written in terms of the electromagnetic field tensor $F_{\mu\nu}$, turns out to be

$$\kappa(t, \rho, z) = 2 \frac{|e| \omega'}{m^3} |E_x(t, \rho, z)| \quad (4)$$

for a counterpropagating geometry, in which case, the interacting gamma quantum is characterized by a wave vector $k' = \omega'(1, 0, 0, -1)$.

In order to take into account bremsstrahlung, the corresponding photon distribution has to be considered. For high energies E_0 of incident bremsstrahlung electrons—which is the case in the present paper as we assume GeV energies—the collimation angle of the emitted photons can be approximated as an inverse Lorentz factor $\theta_\gamma \approx 1/\gamma_e = m/E_0 \sim \mathcal{O}(1)$ mrad. Hence, the vast majority of the produced bremsstrahlung photons is emitted in the direction of propagation of incident electrons. Consequently, the photons energy spectrum can be approximated by [45, 46]

$$I_\gamma(f, \ell) \approx \frac{\ell}{f} \left(\frac{4}{3} - \frac{4f}{3} + f^2 \right) \quad (5)$$

with the normalized photon energy $f = \omega'/E_0$ and the normalized target thickness $\ell = L_T/L_{\text{rad}}$, which relates the target thickness L_T to the radiation length of the material L_{rad} . Note that the formula above is valid within the complete screening approximation and for material with high Z-numbers, as well as for very thin targets with $\ell \ll 1$. Hereafter, a target made up of tungsten is considered with $L_{\text{rad}} = 3.5$ mm and $L_T = 50$ μm , corresponding to $\ell = 0.015$ [13]. In Fig. 2 one sees the bremsstrahlung spectrum per radiating incident electron as given in Eq. (5) for the chosen target thickness as a function of f . We shall assume throughout that the incident electron bunch contains a total (absolute) charge of $Q_e = 10$ pC and that $\delta = 1\%$ of the electrons will emit bremsstrahlung, which represents a reasonable fraction for the chosen target thickness [13]. Accordingly, the total number of radiating electrons is $Q_e \delta / |e| \approx 6 \times 10^5$.

At this point, we can elucidate on the volume V_γ and area A_γ , respectively, occupied by the γ -photons generated from bremsstrahlung. Taking into account that, in the considered experimental setup (see Fig. 1), the incident electron beam spreads over a distance L_{e^-} with the angle θ_{e^-} and that afterwards the generated beam of bremsstrahlung spreads over a distance L to the interaction zone with the angle θ_{rms} , the volume of the γ -photons can be approximated by $V_\gamma \approx 2z_R A_\gamma$, with the cross sectional area

$$A_\gamma \approx \pi(L_{e^-} \theta_{e^-} + L \theta_{\text{rms}})^2, \quad (6)$$

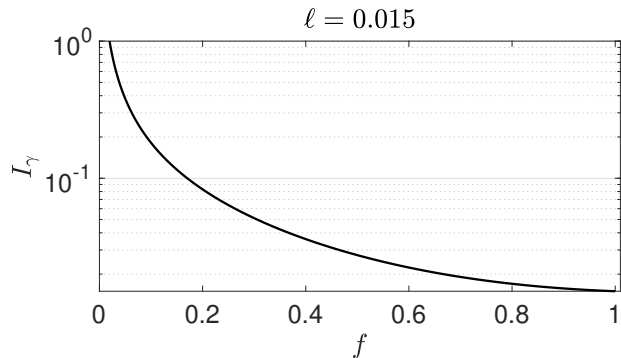


FIG. 2. Bremsstrahlung spectrum as a function of the normalized photon energy $f = \omega'/E_0$ for a target with $\ell = 0.015$.

where $\theta_{\text{rms}} = (\theta_{e^-}^2 + \theta_\gamma^2)^{1/2}$. Here, it is assumed that the electrons are accelerated via laser wakefield acceleration by a portion of the same laser that is used for the pair production. Thus, the longitudinal extension of the electron beam is set to $2z_R$. For further details, we refer to Sec. II A in [33]. In the further course of our consideration the electron beam spreading parameters are set to $L_{e^-} = 10$ cm and $\theta_{e^-} = 0.5$ mrad. The distance to the interaction zone travelled by the γ -photons is taken as $L = 0.5$ m. Accordingly, when the incident electron energy is $E_0 = 2.5$ GeV, the cross sectional area amounts to $A_\gamma \approx \pi(320 \mu\text{m})^2$. It slightly shrinks to $A_\gamma \approx \pi(300 \mu\text{m})^2$ for $E_0 = 10$ GeV, because the beam of γ -photons is less divergent then.

B. Pair production at moderate field strengths: Stable γ -beam model

In the following, we briefly describe the method of Ref. [33] (see especially Secs. IIB and IIC therein) which allows us to calculate the number of created Breit-Wheeler pairs, when both the quantum nonlinearity parameter κ and the laser pulse duration τ are not too large. We denote our corresponding approach as “stable γ -beam model” (S-model in short) for reasons that will become clear in Sec. IIC.

In the considered situation, the number of pairs created by a γ -photon of energy ω' can be estimated directly by integrating the local rate in Eq. (1) over the interaction time T_{int} and interaction volume V_{int} :

$$\mathcal{N}(\omega') \approx \frac{1}{V_\gamma} \int_{V_{\text{int}}} \int_{T_{\text{int}}} R(\kappa)|_{\kappa \rightarrow \kappa(\vec{r}, t)}. \quad (7)$$

Both domains T_{int} and V_{int} are supposed to be determined by the profile of the Gaussian laser pulse (2). Since the latter has no dependence on the azimuthal angle and we assume a counterpropagating beam geometry,

the number of created pairs can be written as

$$\mathcal{N}(\omega') \approx \frac{2\pi}{V_\gamma} \int_{-\infty}^{\infty} dt \int_0^{\infty} \rho d\rho \int_{-t-z_R}^{-t+z_R} dz R(\kappa)|_{\kappa \rightarrow \kappa(t, \rho, z)}. \quad (8)$$

The boundaries of the z -integration take the spatial overlap between laser pulse and bremsstrahlung beam into account (see also Fig. 7 below). In order to include the energy distribution of the bremsstrahlung, an incoherent average of Eq. (8) over the spectrum (5) must be taken. Thus, the number of created Breit-Wheeler pairs per radiating electron in our S-model is given by

$$N_S \approx \int_0^1 df \mathcal{N}(\omega') I_\gamma(f, \ell). \quad (9)$$

Before moving on to the next section we note that the substitution $z = -t - \tilde{z}$ transforms Eq. (8) into

$$\mathcal{N}(\omega') \approx \frac{2\pi}{V_\gamma} \int_{-\infty}^{\infty} dt \int_0^{\infty} \rho d\rho \int_{-z_R}^{z_R} d\tilde{z} R(\kappa) \quad (10)$$

with $\kappa = \kappa(t, \rho, -t - \tilde{z})$. In the transformed expression, the \tilde{z} -integration boundaries are decoupled from the time variable, in contrast to Eq. (8). The performed setting $z = z(t) = -t - \tilde{z}$, which now links the longitudinal component with the time, offers a physical interpretation in semiclassical terms: it describes the (longitudinal coordinate of the) trajectory of a γ -photon moving with the speed of light in negative z -direction. The quantity \tilde{z} correspondingly represents a relative longitudinal offset between different γ -photons. This offset runs between $-z_R$ and z_R , in accordance with the assumed extension of the bremsstrahlung γ -pulse. The picture of point-like γ -photons propagating along classical trajectories will be exploited further in the theoretical model of the next section.

C. Pair production at very high field strengths: Decaying γ -beam model

The method described in Sec. IIB is only applicable when the quantum nonlinearity parameter κ and the laser pulse duration τ are not too large. Otherwise this method will overestimate the pair production yield, because it disregards the attenuation of the γ -rays that arises from their decay into electron positron pairs. In the following we present another calculational method that is able to describe the nonlinear Breit-Wheeler process at κ values substantially exceeding unity. To this end, we adjust the treatment put forward in Ref. [32] and extend it to incorporate γ -rays from bremsstrahlung with a broad frequency spectrum.

While in Sec. IIB the γ -photons were modelled from the beginning by a continuous number density ϱ_γ that interacts with the full spatiotemporal extent of the laser pulse, the approach of the present section relies on the

contributions of individual γ -photons to the pair production. We assume that a γ -photon moves with the speed of light ($c = 1$) along a straight-line trajectory

$$\vec{r}(t) = -t\hat{e}_z + b\hat{e}_\rho \quad (11)$$

where we have set the longitudinal coordinate $z(t) = -t$ antiparallely to the z -axis and introduced a transverse 'impact parameter' b to the origin of the coordinate frame where the center of the laser pulse is located. The longitudinal offset $\tilde{z} = 0$ has been set to zero [see Eq. (10)]. This simplifying assumption, which facilitates the computations, shall be shown below to represent a good approximation in the considered regime of parameters. During its path through the laser field, a γ -photon of energy ω' decays into an electron-positron pair with the probability

$$P(b, \omega') = 1 - \exp \left[- \int_{-\infty}^{\infty} dt R(\kappa) \right]_{\kappa \rightarrow \kappa[\vec{r}(t)]} \quad (12)$$

which coincides with the probability for producing a pair. In the exponent of Eq. (12), the pair production rate $R(\kappa)$ enters, which is evaluated along the trajectory of the γ -photon. Clearly, when the time-integrated rate is much smaller than unity, the exponential can be expanded and one obtains

$$P(b, \omega') \approx \int_{-\infty}^{\infty} dt R(\kappa)|_{\kappa \rightarrow \kappa[\vec{r}(t)]} \quad (13)$$

in accordance with the method of Sec. IIA. However, when the time-integrated rate is not small, which occurs for large values of κ and/or τ , the previous method overestimates the number of created pairs substantially. The reason is that a γ -photon which has decayed into a pair, is lost from the γ beam and cannot induce further pair creation events. Accordingly, the approach of the present section shall be referred to as "decaying γ -beam model" (D-model). Thus, in a situation where Eq. (12) cannot be reduced to Eq. (13), the transition from the process rate to the process probability adopts a nonperturbative form.

The pair production probability $P(b, \omega')$ holds for a γ -photon of energy ω' passing the central point of the laser focus at distance b . In order to obtain the pair yield resulting from an extended beam of bremsstrahlung γ -photons, we first average the individual probability over the transversal interaction area according to

$$\mathcal{P}(\omega') = \frac{2\pi}{A_\gamma} \int_0^{b_{\max}} db b P(b, \omega'). \quad (14)$$

Afterwards, we obtain the total number of produced pairs per radiation electron in the D-model by weighting with the bremsstrahlung spectrum, according to

$$N_D = \int_0^1 df \mathcal{P}(\omega') I_\gamma(f, \ell). \quad (15)$$

For our numerical calculations we cut off the integration domain in Eq. (14) at a sufficiently large upper boundary $b_{\max} = 3w_0$, that corresponds to a cross sectional area of $A_{\max} = \pi(3w_0)^2$. Then we distribute the associated portion of A_{\max}/A_γ bremsstrahlung γ -photons uniformly over the area A_{\max} and calculate the contribution of each trajectory to the pair yield.

III. RESULTS AND DISCUSSION

Based on the S- and D-models described above, our goal in this section is to analyze the physical properties of the strong-field Breit-Wheeler pair production in the overcritical regime with $\kappa > 1$. For our numerical studies, a Ti:Sapphire laser with frequency $\omega = 1.55$ eV is assumed throughout with intensity parameter $\xi \sim \mathcal{O}(100)$ and pulse duration $\tau \sim \mathcal{O}(10)$ fs. Unless specified otherwise, the focal beam waist is chosen as $w_0 = 2$ μm , corresponding to a Rayleigh length $z_R \approx 15.7$ μm . The laser pulse collides with bremsstrahlung γ -photons generated by a few-GeV electron beam of 10 pC total charge. It is assumed that 1% of the incident electrons emit bremsstrahlung, which is a reasonable amount for the chosen target thickness.

A. Comparison between S-Model and D-Model at moderately high field strengths

We begin with presenting the results of numerical calculations performed with the S-model of Sec. II B and the D-model of Sec. II C. Our aim is to compare the obtained pair production yields at moderately high field strengths $\xi \lesssim 100$ and to characterize the borderline of parameters starting from which the D-model needs to be applied because the attenuation of the decaying γ -beam cannot be disregarded anymore.

Figure 3 shows the differential number of created pairs (per radiating electron) in dependence on the normalized bremsstrahlung-photon energy. The set of parameters of a planned experiment on strong-field Breit-Wheeler pair production [13, 33] is considered here: $E_0 = 2.5$ GeV, $\xi = 70$ (corresponding to an intensity of $I \approx 10^{22}$ W/cm²), and $\tau = 30$ fs. The highest value of the quantum nonlinearity parameter resulting in this scenario is $\kappa \approx 2$ for $f \approx 1$. As the figure displays, the contribution to the pair production yields grows monotonously with increasing f . Up to $f \approx 0.5$ (corresponding to $\kappa \approx 1$), the predictions of the S- and D-models closely agree with each other, but start to slightly deviate afterwards. At the bremsstrahlung endpoint $f \approx 1$, the S-model overestimates the pair yields by about 20%.

When the differential pair numbers are integrated over f and multiplied by the number of radiating electrons, we obtain a total yield of ≈ 0.025 pairs per laser shot from the D-model and ≈ 0.028 pairs per laser shot from the S-model. Thus, the γ -beam decay has only a minor impact

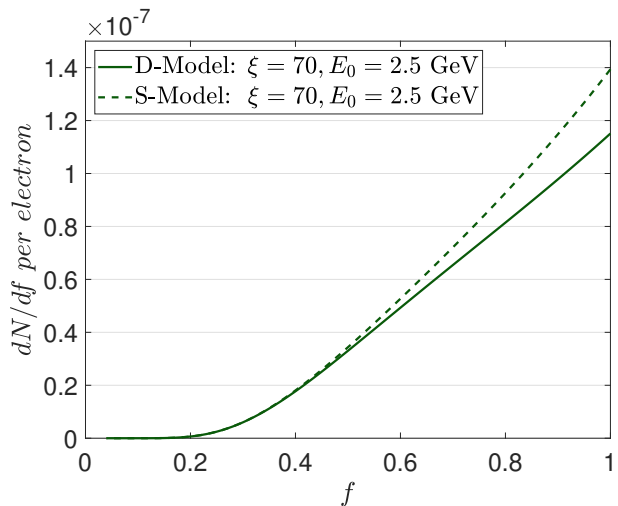


FIG. 3. Comparison between the D-Model (solid) and S-Model (dashed) of differential number of created pairs from different bremsstrahlungs photon energies at $\xi = 70$ and $E_0 = 2.5$ GeV.

on the total yield to be expected in the experiment [13]. Accordingly, the obtained numbers from both the S- and D-model are in good agreement with the pair yield of 0.03 reported in [33]. For later use we note that the S- and D-model predictions for the total yield differ by about 10% in the present example, which is much less than the difference of about 20% arising in the spectrally resolved curves in Fig. 3 at the endpoint $f \approx 1$. The reason is that to the total yield also lower f -values give significant contributions, where S- and D-model lie (much) closer to each other.

When the quantum nonlinearity of the process is enhanced by increasing the incident electron energy, the differences between S- and D-model grow. Using the D-Model for $E_0 = 5$ GeV results in ≈ 0.12 pairs per laser shot (where the S-Model would have given a result of ≈ 0.16) and for $E_0 = 10$ GeV results in ≈ 0.31 pairs per laser shot (where the S-Model would have given a result of ≈ 0.47). Thus, for $E_0 = 5$ GeV, corresponding to a maximal value of $\kappa \approx 4$, the S-model overestimates the pair yield already by about 25%, whereas for $E_0 = 10$ GeV (where $\kappa \lesssim 8$) the yield is overestimated by about 50%. These numbers indicate that the D-model should be utilized for these parameters to obtain quantitatively reliable predictions.

Apart from the value of the quantum nonlinearity parameter κ , we emphasize that also the duration of the interaction influences the relation between S- and D-model predictions. Let us demonstrate this by a simple estimate. In the tunneling-like regime of strong-field Breit-Wheeler pair production at $\kappa \ll 1$, the process rate is given by the analytical expression $R \sim \frac{\alpha m^2 \kappa}{\omega'} e^{-8/(3\kappa)}$. This compact formula still holds approximately for $\kappa \sim 1$ (see, e.g., Fig.5 in [33]). Taking $\kappa = 2$ and $\omega' = 2.5$ GeV, the rate becomes $R \approx 10^{-7} m$. As a consequence, the

time-integrated rate remains smaller than unity for laser pulse durations $\tau \lesssim 10$ fs. Therefore, the S-model is applicable for few-cycle optical laser pulses with duration below 10 fs in this case.

Another interesting aspect in this context is the scaling of the total pair yield with the laser pulse duration. Reducing the previous value from $\tau = 30$ fs to $\tau = 20$ fs, the D-model (S-model) predicts ≈ 0.09 (≈ 0.10) pairs per laser shot for $E_0 = 5$ GeV and ≈ 0.23 (≈ 0.32) pairs per laser shot for $E_0 = 10$ GeV. These results illustrate (via comparison with the corresponding numbers for 30 fs given above) that, to a good approximation, S-model predictions are proportional to the laser pulse duration. However, in a parameter regime, where the use of the D-model is required, the scaling with τ becomes more complex and nonlinear. This distinctive feature is a direct consequence of the different mathematical forms of Eqs. (7) and (12).

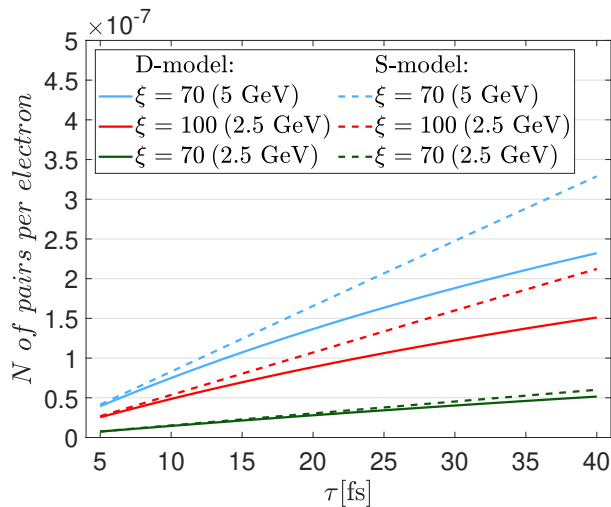


FIG. 4. Dependence of the number of created pairs on the laser duration predicted by the S-model (dashed lines) and the D-model (solid lines) for incident electron energy $E_0 = 5$ GeV at $\xi = 70$ (blue curves), $E_0 = 2.5$ GeV at $\xi = 100$ (red curves) and $E_0 = 2.5$ GeV at $\xi = 70$ (green curves).

The relevance of and scaling with the interaction time is illustrated in Fig. 4. It depicts the number of created pairs in dependence on the laser pulse duration for $E_0 = 2.5$ GeV at $\xi = 70$, $E_0 = 2.5$ GeV at $\xi = 100$, and $E_0 = 5$ GeV at $\xi = 70$. For the S-Model, we observe a linear dependency on the laser duration for both energies, whereas in the D-Model, photon decay while penetrating the laser beam leads to a sublinear growth in the number of pairs with increasing laser duration. For very short pulse durations, the predictions from both models coincide in all three cases. While for $E_0 = 2.5$ GeV and $\xi = 70$, the difference between S- and D-model remains moderate throughout the considered τ -range, the discrepancy grows stronger for larger values of E_0 and ξ . For instance, at $E_0 = 2.5$ GeV and $\xi = 100$ the S-model overestimates the total yield for $\tau = 20$ fs by about 20%,

for $\tau = 30$ fs already by about 30%, and for $\tau = 40$ fs quite sizeably by about 40%. Nearly the same percentage values of relative overestimation by the S-model over the D-model result for the parameter combination $E_0 = 5$ GeV and $\xi = 70$.

B. Pair production in the overcritical field regime

In this subsection, we utilize our D-Model and apply Eq. (15) to obtain several important insights into the Breit-Wheeler pair creation process in the overcritical regime with $1 < \kappa \lesssim 30$. In contrast to the previous Sec. III A, here the attention is put on high laser intensities above 10^{22} W/cm². These values are achievable in the foreseeable future at the laser facilities such as ELI-NP in Romania, where the investigation of the Breit-Wheeler pair production is firmly embedded into the planning [15]. In the following, we shall therefore use a laser pulse duration of $\tau = 20$ fs, as a typical value envisaged at this facility.

1. Spectrally resolved pair yields

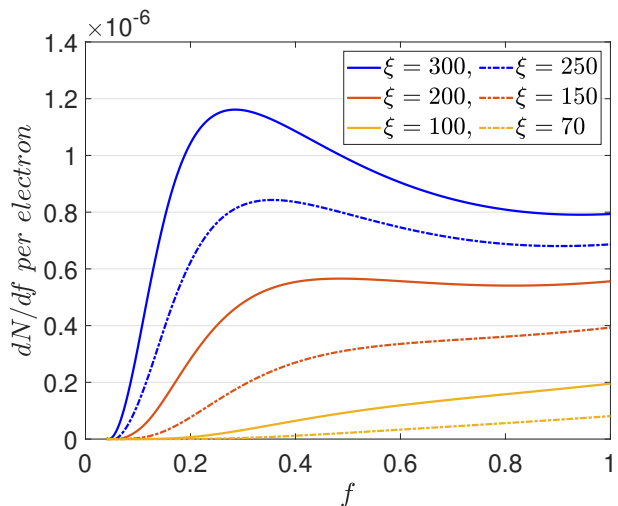


FIG. 5. Differential number of created pairs from different bremsstrahlung photon energies at incident electron energy $E_0 = 2.5$ GeV for different values of the laser intensity parameter $\xi \in \{70, 100, 150, 200, 250, 300\}$ as indicated using the D-model.

By utilizing the D-model we can analyse the contribution to the number of created pairs from different γ -photon energies within the bremsstrahlung spectrum. These contributions are depicted in Fig. 5 for different values of ξ between 70 and 300 at a fixed incident electron energy of $E_0 = 2.5$ GeV. As we go to high values of ξ we see a clear contrast in the distributions compared to the case in Fig. 3. For $\xi = 70$, we observe as before a strictly monotonic increase in the number of created pairs

as f increases. In contrast, for higher values of ξ , a pronounced maximum emerges, indicating a peak contribution at specific γ -photon energies. For $\xi = 150$, the curve shows only a slight bend, while for $\xi = 200$, we observe a global maximum at $f \approx 0.48$. Furthermore there is a maximum at $f \approx 0.36$ for $\xi = 250$ and a very high peak at $f \approx 0.28$ for $\xi = 300$. The formation of those maxima results from three effects which influence the creation of pairs. Firstly, for the parameters under consideration, the local rate of pair creation still approaches to an exponential dependence and thus increases steeply with κ , which is proportional to the product of ξ and f . Thus, for $\xi = 70$, the exponential rate damping is still strong and therefore the number of pairs grows as f increases, whereas for high values of ξ , the field dependence of the rate becomes much flatter (see also Fig. 8 below). Secondly, the number of produced bremsstrahlung photons is much higher for low values of f , as depicted in Fig. 2, which starts playing a crucial role in the pair production when the rate growth has left the very steep exponential region and entered into the flatter portion. Lastly, the exponential decay of the bremsstrahlung photons in the D-model is much more pronounced for high values of κ , which also favors low values of f for the creation of pairs. It is therefore, that we observe the emergence of a maximum at lower values of f , because the increase of the rate with higher values of f is counteracted and eventually overcompensated by the falling distribution of bremsstrahlung photons and their decay for high values of ξ .

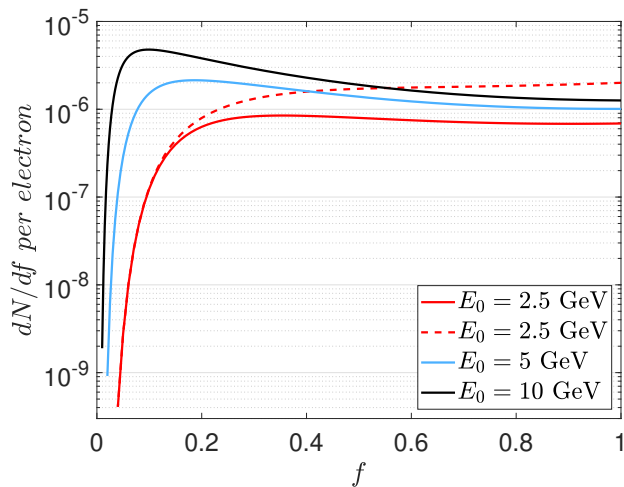


FIG. 6. Contributions to the number of created pairs from different bremsstrahlung photon energies at $\xi = 250$ obtained from the D-model. The red, blue and black curves (in this order) represent different values of the incident electron energy $E_0 \in \{2.5, 5, 10\}$ GeV. The dashed line represents the result for $E_0 = 2.5$ GeV predicted by the S-model.

A similar observation can be made when we compare the impact of the energy of bremsstrahlung photons for different values of the incident electron energy. In Fig. 6

the contribution to the number of created pairs is plotted for $E_0 = 2.5$ GeV (red), $E_0 = 5$ GeV (blue) and $E_0 = 10$ GeV (black) at fixed $\xi = 250$. A global maximum in the number of created pairs arises at $f \approx 0.35$ for $E_0 = 2.5$ GeV, $f \approx 0.185$ for $E_0 = 5$ GeV, and the most pronounced maximum for $E_0 = 10$ GeV at $f \approx 0.0975$.

For comparison, the results predicted by the S-Model for $E_0 = 2.5$ GeV are represented by the dashed red line. It agrees with the D-model result up to $f \approx 0.15$, corresponding to $\kappa \approx 1.1$, but sizably overestimates the yield for higher bremsstrahlung photon energies. In particular, no maximum emerges along the S-Model curve. The S-model results for the higher electron energies are not shown in Fig. 6 because they would deviate even more strongly from the proper pair yields obtained from the D-model. We note that these curves would feature maxima at low f values because of the counteracting trends between the increase of the rate and the decrease of the bremsstrahlung spectrum. An additional effect contained in the D-model description is the attenuation of the γ -beam. In result, the maxima of the blue and black line are located at smaller f values than one would expect based on an S-model consideration.

As an illustration, Fig. 7 depicts the values of the spacetime dependent quantum nonlinearity parameter $\kappa(t, \rho, z, f)$ at $\rho = 0$ for 10 GeV incident electrons and the integration region given in Eq. (8). In the upper panel the local values of κ for very small photon energy with $f = 0.05$ is exposed. Here, the number of created particles is expected to be low as κ is of the order of one. On the other hand, for $f = 0.1$ the values presented in the middle panel overpass the critical value of $\kappa \approx 1$ and the expected pair yield per γ -photon is significantly increased, as the heavy exponential damping characteristic for the tunneling-like regime at $\kappa \ll 1$ is largely softened here, so that the course of the pair production rate is distinctly flattened. This observation combined with the high number of produced bremsstrahlung photons (see the graph in Fig. 2) is responsible for the emergence of the maximum in Fig. 6. Lastly, the quantum nonlinearity parameter for $f = 0.2$ is shown in the lower panel of Fig. 7. Here, $\kappa \approx 6$ is reached leading to a high rate of the particle creation. However, as the number of bremsstrahlung γ 's is much lower than for $f = 0.1$ (see Fig. 2) and their attenuation in the process is stronger, the resulting outcome for particle production is reduced.

2. Total pair yields

In Fig. 8 the total number of pairs produced by a single radiating electron is considered in the intensity range $\xi \in [50, 300]$. Moreover, three different values of the incident electron energy $E_0 \in \{2.5, 5, 10\}$ GeV are studied and depicted as red, blue and black solid lines, correspondingly. It can be seen that the increase in the intensity for the lowest electron energy provides an improvement in the number of created pairs by two orders of mag-

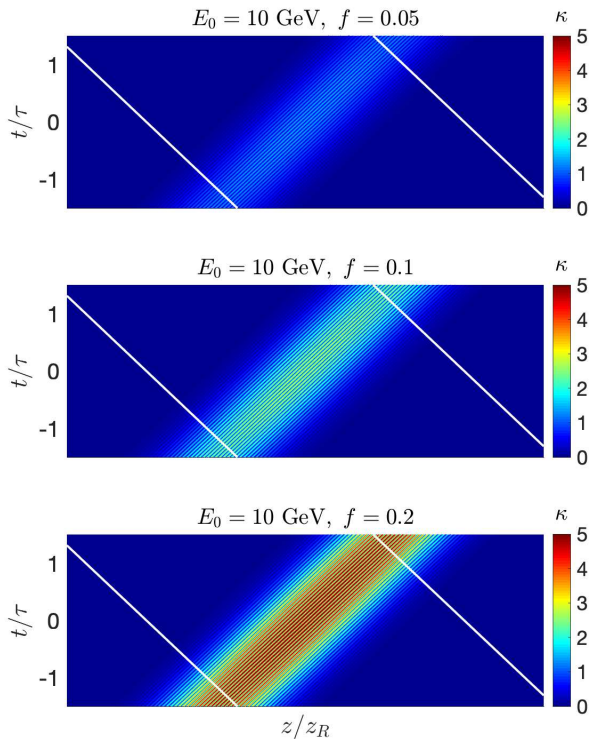


FIG. 7. Time and space dependent quantum nonlinearity parameter $\kappa(t, 0, z, f)$ at the point $\rho = 0$ for photons emitted by 10 GeV electrons at $f = 0.05$ (upper panel), $f = 0.1$ (middle panel) and $f = 0.2$ (lower panel). Moreover, $\xi = 250$ is chosen and the integration region as given in Eq. (8) is encompassed between white lines.

nitude. A pronounced rate growth is also visible, however to a smaller extent, for $E_0 = 5$ GeV and $E_0 = 10$ GeV. The steepest increase occurs up to $\xi \approx 150$, from where on the rate growth becomes significantly flatter.

The S-model would lead to a strong overestimation of the rate practically throughout the whole range of considered laser intensities. This is illustrated by the red dashed line for $E_0 = 2.5$ GeV. It approximately agrees with the D-model rate up to $\xi \approx 70$, which is associated with a maximal $\kappa \approx 2.1$, and strongly deviates for the higher intensities. The deviations to the D-model prediction would be even larger for the higher incident electron energies, which are therefore not included in the figure.

At this point we emphasize that the κ values, for which the S- and D-models coincide, are lower for the spectrally resolved pair yields (see discussion of Figs. 3 and 6) than for the total pair yields. As already mentioned before this is because one integrates over the spectrally resolved curve in order to get the total pair yield, thus including also those parts of the bremsstrahlung spectrum where both models are in good agreement.

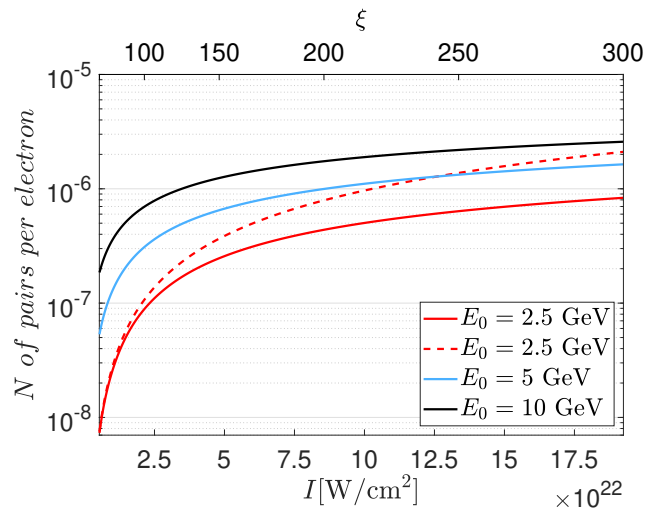


FIG. 8. Dependence of the number of created pairs on the laser intensity for various incident electron energies, color-coded with red, blue and black solid lines for $E_0 = 2.5$, 5, and 10 GeV using the D-model. The dashed line represents the result for $E_0 = 2.5$ GeV given by the S-model.

The total pair yield in an envisaged experiment can be obtained by taking the number of interacting γ -photons into account. As mentioned above, we assume that the incident electrons come in bunches of 10 pC total charge and that 1% of them will emit bremsstrahlung. Thus in the range $\xi \in [50, 300]$, for $E_0 = 2.5$ GeV, from 0.005 to 0.52 pairs per shot can be expected, depending on the applied intensity. Next, by increasing the incident electron energy to 5 GeV [47], the pair yield can be amplified significantly to 0.03 to 1.02 pairs per shot. Lastly, the amount of 0.11 and up to 1.61 created positrons is achievable in the most optimistic scenario with $E_0 = 10$ GeV. Furthermore if we compare the yield between 2.5 GeV and 5 GeV, we observe a fourfold raise in the number of created particles at $\xi = 100$ from 0.055 pairs to 0.19 pairs per shot. At $\xi = 250$, doubling the energy from 2.5 GeV to 5 GeV still results in approximately doubling the yield, increasing from 0.40 pairs per shot to 0.83 pairs per shot. For 10 GeV we observe 0.44 pairs at $\xi = 100$ and up to 1.37 created pairs for $\xi = 250$. Hence, the numbers presented here drastically outperform the predictions for 'discovery experiments' planned in the nearest future (see Sec. III A) and would thus allow for precision tests of the underlying theory.

At this point, we can quantify the appropriateness of the approximation in Eq. (11) where the longitudinal offset in the γ -photon trajectory was set to zero, $\tilde{z} = 0$. It means that the considered γ -photons reach the center of the laser focus at time $t = 0$, where the laser field strength is maximum. When the trajectory is taken more generally as $\vec{r}(t) = -t\hat{e}_z + \tilde{z} + b\hat{e}_\rho$, those γ -photons with $\tilde{z} > 0$ ($\tilde{z} < 0$) hit the laser pulse maximum by $\hat{t} = \tilde{z}/2$ earlier (later). An average over the relevant range of \tilde{z} -values would need to be taken in a more accurate treatment to

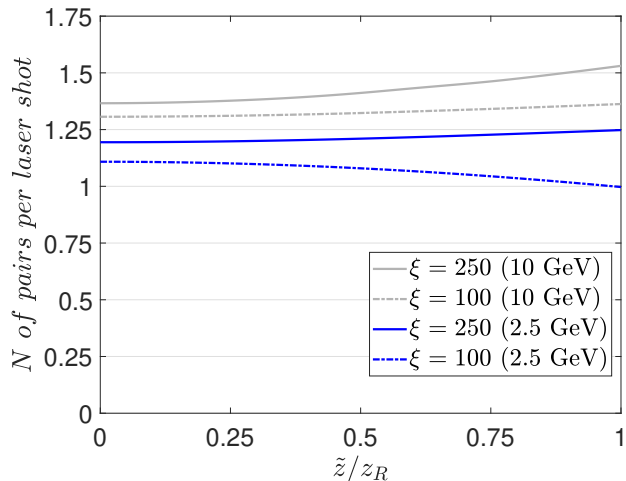


FIG. 9. Number of created pairs per laser shot as a function of the relative offset of the γ -photon trajectories for different values of $\xi \in \{100, 250\}$ at $E_0 = 2.5$ GeV and 10 GeV. For presentation purposes the lowest curve was scaled by an amplification factor of 20, and the two curves in the middle were amplified by a factor of 3. The considered maximum offset coincides with the upper boundary of our integration region [see e.g. Eq. (10)].

calculate the pair yield from a bremsstrahlung γ -burst. The dependence of the total number of produced pairs per laser shot on the longitudinal offset is depicted in Fig. 9 for $0 \leq \tilde{z} \leq z_R$. One can see that the curves are very flat, implying that it is not strictly necessary to take an average; accordingly, the simplifying assumption $\tilde{z} = 0$ in Eq. (11) works well in the considered range of parameters. The largest relative differences arise for $E_0 = 2.5$ GeV and $\xi = 100$, where the pair yield is reduced by about 2.5% (10%) when $\tilde{z} = z_R/2$ ($\tilde{z} = z_R$); for $E_0 = 10$ GeV and $\xi = 250$ the pair yield is instead increased by about 3% (12%) for the same values of \tilde{z} . The approximation works well for both large values of ξ as well as large values of E_0 .

The reason for the slight decrease or increase of the pair number for larger \tilde{z} is that the laser pulse is then hit by the γ -ray when its center has passed the focal point. The correspondingly reduced field intensity leads to a decrease of the pair number for $\xi = 100$, $E_0 = 2.5$ GeV where the value of κ is still moderate and the behavior of the production rate is exponential-like. Instead, for large $\kappa \gg 1$, the rate $R(\kappa)$ grows only rather slowly, so that the reduction of the field intensity plays a minor role. Here, the enhanced interaction volume, associated with the transversally broadened extension of the laser pulse, causes the dominant effect, leading to an increase of the pair number.

In result, when averaging over the offsets, we see only very slight deviations in the yield compared to the approximated case: For $E_0 = 2.5$ GeV the resulting yield is lower by about 3.4% for $\xi = 100$ and higher by about only

1.6% for $\xi = 250$ than its value at $\tilde{z} = 0$. For $E_0 = 10$ GeV the yield increases by about 1.6% for $\xi = 100$ and by about 4.2% for $\xi = 250$. From this we see that our simplification gives valid results.

The influence of tighter or looser laser focusing is displayed in Fig. 10. To that end, the energy of the laser pulse

$$E_L \propto \xi^2 w_0^2 = \left(\frac{250}{x}\right)^2 (2x \mu\text{m})^2 = \text{constant} \quad (16)$$

is kept constant and the parameter x is varied between 0.5 and 6.5, leading to higher intensity accompanied by narrower beam waist and visa versa. Accordingly, the scaled intensity parameter $\xi = 250/x$ in the range [39, 500] with the corresponding beam radius $w_0 = 2x \mu\text{m}$ in the intervall [$1 \mu\text{m}$, $13 \mu\text{m}$] was studied for the incident electron energies $E_0 = 2.5$ GeV (red), $E_0 = 5$ GeV (blue) and $E_0 = 10$ GeV (black). Additionally the prediction by the S-Model is displayed for $E_0 = 2.5$ GeV (red dashed) for comparison. Starting from $x \approx 3.5$, corresponding to a maximal $\kappa \approx 2.1$, both models closely coincide with each other.

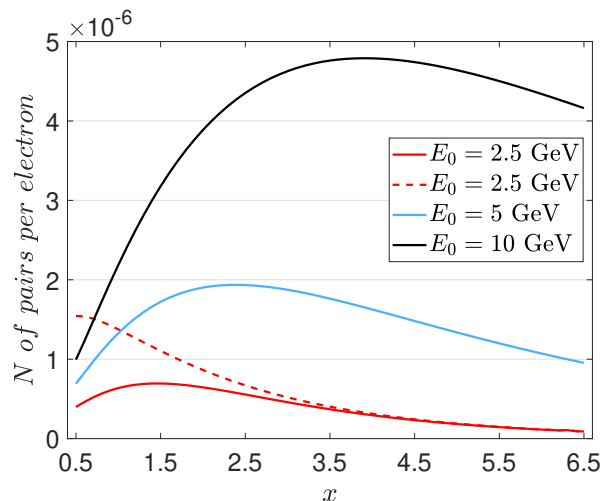


FIG. 10. Number of pairs as a function of the degree of laser focusing obtained by setting $\xi = 250/x$ and $w_0 = 2x \mu\text{m}$ and keeping the laser energy constant. The black, blue and red solid lines represent different values of the incident electron energy $E_0 \in \{2.5, 5, 10\}$ GeV using the D-model, while the dashed line results from the S-model for $E_0 = 2.5$ GeV.

Interestingly, the D-model outcomes show optimal values for the focusing with maximum yield at $x \approx 1.5$ for $E_0 = 2.5$ GeV, at $x \approx 2.4$ for $E_0 = 5$ GeV and at $x \approx 3.9$ for $E_0 = 10$ GeV. On the one hand one might have naively expected that higher ξ and therefore higher intensities would always lead to higher yields, as depicted in Fig. 8 because of the exponential dependency of the rate which rises steeply when ξ grows. But on the other hand the interaction volume decreases for smaller x , so that fewer γ photons can participate in the creation of pairs; this effect scales quadratically with x . For moderate values of

κ , the x -dependence of the pair yield is dominated by the dependency of the rate. But for a parameter range where κ largely exceeds 1, the rate dependency is distinctly flattened and both counteracting effects can compete with each other. Additionally, there is the feature of the D-Model that γ -photons penetrating the laser pulse decay over time which further reduces the normally beneficial effect of higher intensities on the yield (see Fig. 8 and Fig. 6). This leads to an even greater necessity for a large interaction volume and correspondingly decreased laser intensity, because then the influence of the photon decay is reduced. In summary, maximum focusing is not recommended, but instead it is advised to aim for specific focusing depending on the incident electron energy to maximise the number of created pairs.

Finally, we draw a comparison with the S-Model. Since this model does not take the γ -beam decay into account, its predicted balancing of the influence of higher intensity versus larger interaction volume happens at higher degrees of laser focusing than in the D-model. As the dashed red curve in Fig. 10 indicates, the maximum predicted by the S-Model for $E_0 = 2.5$ GeV lies at $x \approx 0.5$. Furthermore the S-Model would yield a maximum at $x \approx 1$ for $E_0 = 5$ GeV and at $x \approx 2$ for $E_0 = 10$ GeV (not shown). By comparison with the corresponding D-model predictions we see that significantly weaker focusing leads to optimum pair yields, when the decay of the γ -beam is properly taken into account. This is because the decay feature, that leads to a reduction of the pair production relative to the S-model approach, is less pronounced when the field intensity is not too high. A more extended interaction region with somewhat reduced peak intensity is therefore more beneficial.

It is interesting to note that the obtained positions of the focusing optimum in the S-model are proportional to E_0 and thus correspond to a common maximal value of $\kappa \approx 15$ for all three electron energies. Instead, in the D-model, the location of the maxima grows sublinearly with the increase of E_0 . This behaviour of the D-model—which at first sight might appear surprising, given its characteristic preference for not too high intensities—can be attributed to the mainly contributing range of γ -photon energies. In Fig. 6 we saw the emergence of a global maximum in the spectrally resolved number of created pairs, which shifts to lower values of f , and thus to lower κ values when E_0 increases. This trend may explain why the relative growth of the optimum focusing degree expressed by the parameter x occurs more slowly in the D-model than the S-model. Nevertheless, on an absolute scale, the optimum x -values are substantially larger in the D-model than the S-model, corresponding to considerably less tight focusing, as described above.

IV. CONCLUSIONS

Nonlinear Breit-Wheeler pair production in collisions of a focussed high-intensity laser pulse with a beam of high-energy γ -photons from bremsstrahlung has been discussed in the overcritical regime $1 < \kappa \lesssim 30$, which will be achievable at the next generation laser facilities with intensities of $\sim 10^{23}$ W/cm². The presented results complement our previous study [33] of the intermediate interaction regime around $\kappa \approx 1$. To this end, a theoretical model was used that accounts for the attenuation of the bremsstrahlung beam due to the pair production process. The model coincides with our previous approach in the limit of moderate laser intensities and short pulse durations, but also applies to the overcritical regime.

It was shown that in an experiment combining bremsstrahlung γ -photons emitted from an incident 10 pC beam of 10 GeV electrons with a 20 fs, 10^{23} W/cm² laser pulse, more than one pair could be generated per shot, which would allow for precision measurements with increased statistical accuracy and deeper understanding of the underlying vacuum structure. That means, if the repetition rate of the laser system is 0.1 Hz, one could produce 360 pairs per hour. The scaling of the pair yield with laser pulse duration was found to be sublinear, because of the γ -beam decay. Moreover, regarding the impact of bremsstrahlung photons from different parts of the spectrum it was shown that, in contrast to Ref. [33], also γ -photons of relatively low energy play an important role in the particle creation. Accordingly, by the considered setup a rather broad range of κ values is probed simultaneously. Finally, the impact of the laser focusing at fixed laser pulse energy was elucidated, with the outcome that in the overcritical regime there is an optimal focal spot size: Beyond this point, focusing even more tightly to reach higher peak intensity would reduce the pair production yield.

As a general result it has thus been shown that interesting properties of pair creation in the overcritical field regime arise from the relatively slow growth of the production rate with increasing laser intensity: While for small and intermediate values $\kappa \lesssim 1$, the optimum pair yield is known to be achieved for the highest bremsstrahlung energies and the tightest laser focussing, in the considered overcritical regime it is instead more beneficial to relax these conditions in a suitable manner.

ACKNOWLEDGMENTS

This work has been funded by the Deutsche Forschungsgemeinschaft (DFG) under Grant No. 392856280 within the Research Unit FOR 2783/2.

[1] F. Sauter, Z. Phys. **69**, 742 (1931).

[2] H. R. Reiss, J. Math. Phys. **3**, 59 (1962).

- [3] A. I. Nikishov and V. I. Ritus, Zh. Eksp. Teor. Fiz. **46**, 776 (1963) [JETP Lett. **19**, 529 (1964)].
- [4] A. I. Nikishov and V. I. Ritus, Zh. Eksp. Teor. Fiz. **52**, 1707 (1967) [JETP Lett. **25**, 1135 (1967)].
- [5] H. R. Reiss, Phys. Rev. Lett. **26**, 1072 (1971).
- [6] V. S. Popov, Pis'ma Zh. Eksp. Teor. Fiz. **13**, 261 (1971) [JETP Lett. **13**, 185 (1971)]; Yad. Fiz. **19**, 1140 (1974) [Sov. J. Nucl. Phys. **19**, 584 (1974)].
- [7] A. A. Grib, V. M. Mostepanenko, and V. M. Frolov, Theor. Math. Phys. **13**, 1207 (1972); V. M. Mostepanenko and V. M. Frolov, Yad. Fiz. **19**, 885 (1974) [Sov. J. Nucl. Phys. **19**, 451 (1974)].
- [8] V. I. Ritus, J. Sov. Laser Res. **6**, 497 (1985).
- [9] A. Di Piazza, C. Müller, K. Z. Hatsagortsyan, and C. H. Keitel, Rev. Mod. Phys. **84**, 1177 (2012).
- [10] A. Fedotov, A. Ilderton, F. Karbstein, B. King, D. Seipt, H. Taya, G. Torgrimsson, Phys. Rep. **1010**, 1 (2023).
- [11] D. L. Burke *et al.*, Phys. Rev. Lett. **79**, 1626 (1997).
- [12] S. Meuren, Probing strong-field QED at FACET-II (SLAC E-320), [https://conf.slac.stanford.edu/facet-2-2019/sites/default/files/basic-page99docs/sfqed_036008](https://conf.slac.stanford.edu/facet-2-2019/sites/default/files/basic-page99docs/sfqed_2019-09-10-facet-slac-stanford-equity-phys-base-page99docs/sfqed_036008) (2019).
- [13] F. C. Salgado *et al.*, New J. Phys. **23**, 105002 (2021).
- [14] H. Abramowicz *et al.*, Conceptual design report for the LUXE experiment, Eur. Phys. J. Spec. Top. **230**, 2445 (2021).
- [15] I. C. E. Turcu *et al.*, Rom. Rep. Phys. **68**, S145 (2016); <http://www.eli-np.ro/e6.php>
- [16] T. Heinzl, A. Ilderton, and M. Marklund, Phys. Lett. B **692**, 250 (2010).
- [17] K. Krajewska, J. Z. Kamiński, Phys. Rev. A **86**, 052104 (2012).
- [18] A. I. Titov, H. Takabe, B. Kämpfer, and A. Hosaka, Phys. Rev. Lett. **108**, 240406 (2012).
- [19] S. Villalba-Chavez, C. Müller, Phys. Lett. B **718**, 992 (2013).
- [20] S. Meuren, K. Z. Hatsagortsyan, C. H. Keitel, and A. Di Piazza, Phys. Rev. D **91**, 013009 (2015).
- [21] M. J. A. Jansen, J. Z. Kamiński, K. Krajewska, and C. Müller, Phys. Rev. D **94**, 013010 (2016).
- [22] Q. Z. Lv, S. Dong, Y. T. Li, Z. M. Sheng, Q. Su, and R. Grobe, Phys. Rev. A **97**, 022515 (2018).
- [23] A. I. Titov, B. Kämpfer, Eur. Phys. J. D **74**, 218 (2020).
- [24] Y. Lu, N. Christensen, Q. Su, and R. Grobe, Phys. Rev. A **101**, 022503 (2020).
- [25] D. Seipt and B. King, Phys. Rev. A **102**, 052805 (2020).
- [26] T. Heinzl, B. King, A. J. MacLeod, Phys. Rev. A **102**, 063110 (2020).
- [27] F. Wan, Y. Wang, R. T. Guo, R. R. Chen, R. Shaisultanov, Z. F. Xu, K. Z. Hatsagortsyan, C. H. Keitel, and J. X. Li, Phys. Rev. Research **2**, 032049(R) (2020).
- [28] T. Podszus, V. Dinu, A. Di Piazza, Phys. Rev. D **106**, 056014 (2022).
- [29] P. Chen and L. Labun, Phys. Plasmas **30**, 083302 (2023).
- [30] N. Mahlin, S. Villalba-Chávez and C. Müller, Phys. Rev. D **108**, 096023 (2023).
- [31] A. Di Piazza, Phys. Rev. Lett. **117**, 213201 (2016).
- [32] A. Mercuri-Baron *et al.*, New J. Phys. **23**, 085006 (2021).
- [33] A. Golub, S. Villalba-Chávez, C. Müller, Phys. Rev. D **105**, 116016 (2022).
- [34] A. Eckey, A. Golub, F. C. Salgado, S. Villalba-Chávez, A. B. Voitkiv, M. Zepf and C. Müller, Phys. Rev. A **110**, 043113 (2024).
- [35] T. G. Blackburn, M. Marklund, Plasma Phys. Controlled Fusion **60**, 054009 (2018).
- [36] A. Eckey, A. B. Voitkiv, C. Müller, Phys. Rev. A **105**, 013105 (2022).
- [37] A. Eckey, A. B. Voitkiv, C. Müller, Phys. Rev. A **105**, 013105 (2022).
- [38] A slightly different mechanism for efficient generation of γ -rays has been considered in A. J. MacLeod, P. Hadjisolomou, T. M. Jeong, and S. V. Bulanov, Phys. Rev. A **107**, 012215 (2023).
- [39] B. King and S. Tang, Phys. Rev. A **109**, 032823 (2024).
- [40] J. W. Yoon *et al.*, Optica **8**, 630 (2021); see also <https://corels.ibs.re.kr>.
- [41] V. I. Ritus, Ann. Phys. (N.Y.) **69**, 555 (1972); N. B. Narozhny, Phys. Rev. D **21**, 1176 (1980).
- [42] T. Blackburn, A. Ilderton, M. Marklund, and C. Ridgers, New J. Physics **21**, 053040 (2019).
- [43] C. Baumann, E. N. Nerush, A. Pukhov, and I. Yu. Kostyukov, Sci. Rep. **9**, 9407 (2019).
- [44] Y. I. Salamin, Appl. Phys. B **86**, 319 (2007).
- [45] Y.-S. Tsai, Rev. Mod. Phys. **46**, 815 (1974).
- [46] P. A. Zyla *et al.*, (Particle Data Group), Prog. Theor. Exp. Phys. **8** (2020).
- [47] H. T. Kim *et al.*, Appl. Sci. **11**(13), 5831 (2021).